Stabilization of Cu nanostructures by grain boundary doping with Bi: Experiment versus molecular dynamics simulation

S. G. Mayr* and D. Bedorf
I. Physikalisches Institut, Georg-August-Universität Göttingen, Friedrich-Hund-Platz 1, 37077 Göttingen, Germany
(Received 22 October 2006; revised manuscript received 22 March 2007; published 20 July 2007)

Coarsening of nanocrystalline systems at elevated temperatures can be prevented by adding small amounts of impurities to grain boundaries and interfaces, as found in a variety of instances. For the model systems CuBi and CuAg we investigate atomic-scale mechanisms, which underlie stabilization of the nanophase in the presence of an open surface, using experiments, molecular dynamics computer simulations, and thermodynamic considerations. We find that the occurrence of locally negative grain boundary free energies due to dopants is sufficient to frustrate grain growth via a metastable equilibrium. Our treatment can be generalized to other systems with grain boundary segregation.

DOI: 10.1103/PhysRevB.76.024111 PACS number(s): 61.46.Hk, 68.03.Hj, 68.35.Dv, 68.55.−a

I. INTRODUCTION

Although nanoscale structured materials have become widely available in modern science and technology (e.g., Ref. 1 and references therein), their thermal stability remains still a major issue of concern:[2] The inherent presence of a high portion of interfaces (viz., surfaces and grain boundaries) may lead to coarsening, unless (i) appropriate kinetic constraints are imposed, or (ii) the nanosystem resides in a thermodynamic (meta)stable state, as manifested by a (local) minimum of the Gibbs free energy. In the case of nanocrystalline metal and semiconductor systems, both approaches (i) and (ii) can basically be realized by the addition of small amounts of impurity atoms, which segregate to the grain boundaries,[3] while the distinction between grain boundary drag effects[4] and a thermodynamic stabilization by a reduction of the grain boundary free energy[5,6] remains less clear in experiments,[7–9] and is still under debate.[10]

For more than 130 years[11] CuBi has been known as a paradigm of a strongly phase-separating[12,13] system; specifically aligned Cu grain boundaries of *bulk* polycrystalline samples with some tens of ppm of Bi at temperatures mostly between the solidus and liquidus lines have been investigated extensively during recent years with respect to segregation,[14,15] faceting,[16–18] embrittlement,[19–21] and phase transitions[22,23] in experiments and computer simulations. To wrap up the most important tendencies for the present work, grain boundary segregation—sometimes accompanied by faceting[19]—has been reported for low enough temperatures and Bi concentrations far within the solid regions of the Cu-Bi phase diagram,[18] while grain boundary prewetting and wetting have been observed close to and beyond the bulk solidus lines, respectively.[22,23] Excellent reviews on these topics may be found in the above-mentioned references. Within this context it is interesting to mention that the segregation strength has been shown to scale with the Gibbs free energy of the original grain boundary.[14]

The atomic-scale mechanisms that underlie embrittlement of Cu grain boundaries when doped with Bi were recently controversially debated, based on two contradictory *ab initio* calculations.[20,21] The notion[21] that the size mismatch of Bi and Cu plays a key role is compatible with previous *ab inito* calculations as well as the possibility of realistically describing CuBi with a Finnis-Sinclair[24] (FS) type of potential.[25–27]

The literature survey above illustrates that the CuBi system is extremely well characterized, and consequently an ideal testbed to investigate the mechanisms of grain-boundary-segregation-induced stabilization of nanostructures—using systematic experiments and computer simulations. This is achieved by employing nanocrystalline thin Cu and $Cu_{99}Bi_1$ films, which are prepared by cocondensation and subsequently annealed to investigate grain growth. The experiments are interpreted and compared to classical molecular dynamics (MD) simulations on equilibrium segregation and grain growth in nanocrystalline Cu, CuBi, and CuAg systems. As a key issue, we will address the question whether thermodynamics or kinetics is responsible for the dramatic slowing down in grain growth upon addition of Bi dopants to the grain boundaries. Previous simulation studies in this area focused on the structure in specific CuBi grain boundaries[25–27] or grain growth in two-dimensional Lennard-Jones systems,[28] which lack direct comparability to the physics occurring in metals in three dimensions.

The paper is organized as follows. After reviewing the experimental and simulation details in Sec. II, we present the results of experiments and simulations in Secs. III and IV, respectively. After a thermodynamic discussion in Sec. V, we conclude in Sec. VI.

II. EXPERIMENT AND SIMULATION DETAILS

Nominally 100-nm-thick Cu and $Cu_{99}Bi_1$ thin films were deposited at room temperature onto thermally oxidized SiO_2 wafers using ultrahigh-vacuum electron beam evaporation (base pressure: $\lesssim 1.2\times10^{-10}$ mbar), as described before.[29] After deposition, the films were optionally annealed *in situ* for $\approx$22 min, at 473 K, which proved to be sufficient to induce bismuth diffusion in a previous investigation.[30] Directly after venting the chamber, the surface grain sizes of the samples were characterized with atomic force microscopy (AFM) in tapping mode. This approach ensured that oxide contaminations could greatly be excluded.[31]

Additionally, cross-sectional $Cu_{99}Bi_1$ samples were prepared for transmission electron microscopy (TEM) using the

standard sandwich technique, employing hot polymerizing glue (2 h at 403 K), mechanical grinding, and ion etching; the cross sections were characterized by the usual bright field technique as well as with respect to composition, using energy-dispersive x-ray (EDX) measurements. Additional experimental studies, including x-ray photoelectron spectroscopy (XPS) studies of the surface composition, x-ray diffraction (XRD), and a systematic variation of the Bi content, will be presented in more detail elsewhere.[32]

To access the thermodynamics and kinetics during grain growth of Cu nanograins in the presence of Bi and—for comparison—Ag impurities in detail, classical MD simulations are performed in three dimensions. The interaction potentials were based on the FS and embedded atom method[33] formalism, using the highly realistic parametrizations of Yan *et al.*[26] for CuBi and Foiles *et al.*[34] for CuAg, respectively. In particular, the CuBi potential has been fitted to show excellent agreement with experiments[25,26] and *ab initio* simulations[27] with respect to grain boundary structure, elastic constants, and thermal properties, while also the CuAg potential is well established to describe grain boundaries and interfaces.[35,36] The dilute-limit enthalpies of mixing of Bi in single-crystalline Cu were determined to decrease only slightly as a function of temperature [ΔH_{mix}(473 K) $=1.63$ eV/atom, ΔH_{mix}(673 K)$=1.47$ eV/atom, and ΔH_{mix}(873 K)$=1.41$ eV/atom], choosing crystalline (for 473 K) and liquid (for 673 and 873 K) Bi reference states. For Ag impurities in Cu we obtain $\Delta H_{mix}=0.155\pm0.003$ eV/atom in the solid state, while in the liquid state the heat of mixing vanished almost completely for CuBi and CuAg, as expected for alloys with dominant size mismatch of the constituents.

In addition it is very instructive in the present context to consider the surface and interface energies γ_S and γ_I in the Cu-Bi system. For the (111) Cu surface, which is the predominant texture in thin film samples in fcc systems, we calculate almost independently of temperature that $\gamma_S=0.90\pm0.03$ N/m, which is reduced further when covered with Bi: For a monolayer of Bi on top of Cu (111) we find for the sum of the Bi surface and Cu-Bi interface energies (viz. $\gamma_S+\gamma_I$) 0.78 N/m for 473 K and 0.73 N/m for 673 and 873 K, when compared with the corresponding infinite equilibrium bulk phases. Thus the present potential also correctly accounts for the experimentally observed surface segregation.[15]

During MD simulations the classical multiparticle problem is solved by employing a fifth-order Gear predictor-corrector scheme, while isothermal and isobaric conditions are obtained using Berendsen[37] types of thermostats and barostats, respectively,[38] with periodic boundaries employed in all spatial directions. As a starting point, simulation cells containing 27 Cu grains (grain size $\approx$6 nm diameter) and 474 371 atoms total are generated using a Voronoi construction,[41] and subsequently densified at 1 GPa hydrostatic pressure, before zero pressure is attained at the desired temperatures, which we choose below (473 K) and above (673 K) the solidus line, as well as in the grain boundary wetting regime (873 K) of the targeted CuBi systems.

Enthalpically favorable substitutional sites within grain boundaries are identified by the high volume of their corresponding Wigner-Seitz cells,[42] while the enthalpies are extracted directly from the energy changes of the MD cell upon doping at $p=0$. On these sites, Cu atoms are subsequently replaced by Bi or Ag, following the desired statistical distribution, as described in Sec. IV in more detail. Simultaneous occupation of directly neighboring sites was excluded, after test calculation revealed strongly elevated energies under these conditions. The temporal evolution of microstructure was investigated by monitoring the internal system energy, volume, and portion of grain boundary atoms. The latter were identified by employing the structural order parameter P_{st}, as introduced by Zhu *et al.*:[44]

$$P_{st}(k)=\sqrt{\frac{\sum_i[\theta_k(i)-\theta_k^p(i)]^2}{\sum_i[\theta_k^u(i)-\theta_k^p(i)]^2}}. \quad (1)$$

Here, $\theta_k(i)$ denotes the ith smallest angle formed with atom k at the vertex and any pair of its n_{nb} nearest neighbor atoms, θ_k^p is the same quantity for the perfect lattice, and $\theta_k^u(i)=2\pi i/n_{nb}(n_{nb}-1)$ is the uniform angular distribution, where $n_{nb}=12$ is chosen to be the number of neighbors in a perfect fcc lattice. The distribution of P_{st} around a grain boundary starts significantly at $P_{st}\gtrapprox0.32$ and shows a maximum at $P_{st}\approx0.4$, reaching up to $P_{st}\approx0.6$. Visual inspection indicates that atoms with $P_{st}>0.4$ can be regarded in good approximation as grain boundary atoms, while those with $P_{st}<0.4$ are located within either the grain or the transition region between grain and grain boundary. We therefore identify the number of grain boundary atoms, N, with the amount of atoms with $P_{st}>P_{st,c}$ ($P_{st,c}=0.4$) within the simulation cell. Based on this definition, reduction of N could basically still results from two different effects, i.e., (i) grain growth and (ii) grain boundary relaxation. However, test calculations during dramatic grain boundary relaxation and densification when annealing *as constructed* Voronoi polycrystals for the first time at elevated pressures and temperatures revealed only a minor influence of (ii) on N for our specific choice of $P_{st,c}$.[45] Considering N a reasonable measure to quantify grain boundary area $S\propto N$, it is interesting to note that, within stereology, S/V is equal to $2/\bar{l}$, where V is the volume of the simulation cell and $\bar{l}$ denotes the experimentally accessible average grain intercept length.[46]

III. EXPERIMENTAL RESULTS

The surface topographs of Cu and $Cu_{99}Bi_1$ films before and after annealing in Fig. 1 show the occurrence of significant surface grain growth only in the case of pure Cu films. The addition of small amounts of Bi clearly inhibits coarsening of the surface grains during annealing, and is accompanied by segregation of at least a Bi monolayer to the surface, as inferred from XPS measurements. However, to fully understand this phenomenon it is necessary to consider the microstructure and composition beyond the surface, i.e., within the film. Cross-sectional TEM and EDX measurements after annealing of $Cu_{99}Bi_1$ in Fig. 2 show that temperature treatment leads to a compositional and morphologi-

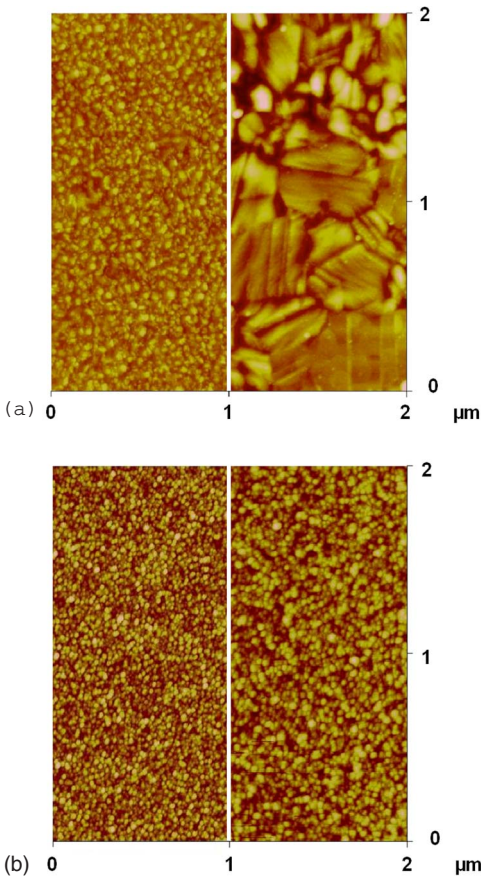

FIG. 1. (Color online) Evolution of surface grains during annealing at 473 K for 22 min in (a) pure Cu and (b) $Cu_{99}Bi_1$. The left parts of the images correspond to AFM surface topographs before annealing. The overall height scale is 10 nm.

cal heterogeneity inside the films: Grains far apart from the film interfaces show coarsening, accompanied by a decreasing Bi content. The microstructure close to interfaces, on the other hand, is highly preserved at increasing Bi concentrations.

IV. SIMULATION RESULTS

As the experimental results in Sec. III indicate, the addition of a sufficient amount of Bi dopants to grain boundaries of nanocrystalline Cu is capable of preventing microstructure from coarsening; it remains stable in coexistence with a Bi surface segregation layer of at least one monolayer thickness at temperatures of at least 473 K. To address the energetics and kinetics of this phenomenon on the atomic scale, MD simulations on the addition of Bi (and—for comparison—Ag) dopants of nanocrystalline Cu are performed and the impact on grain growth is investigated.

As a starting point it is first necessary to estimate the concentration of grain boundary dopants in the presence of an open surface *before* grain growth has occurred. This requires a detailed knowledge of the enthalpies of mixing as a function of the number of substitutional atoms within the grain boundaries. Proceeding as detailed in Sec. II, we

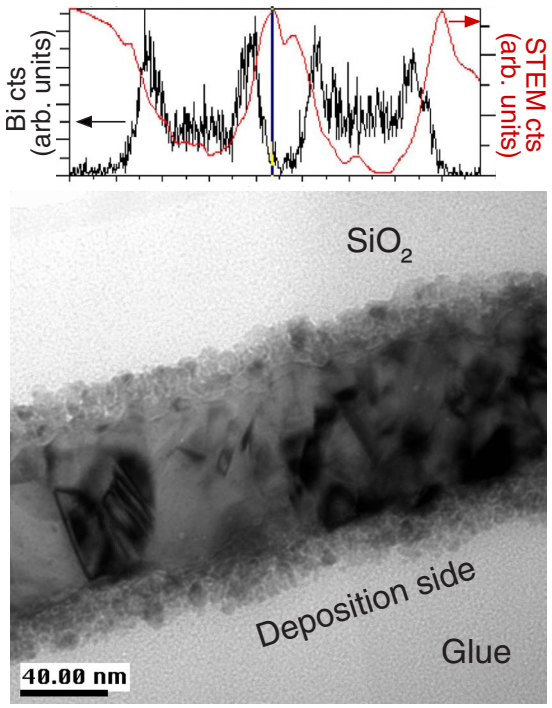

FIG. 2. (Color online) Bottom: Cross-sectional bright-field TEM measurement of a $Cu_{99}Bi_1$ film after annealing at 473 K for 22 min. Clearly, a nanocrystalline structure is preserved at the surface and SiO_2 interfaces. Top: Cross-sectional EDX (left axis) and scanning transmission electron microscopy (STEM) (right axis) measurements of the $SiO_2/Cu_{99}Bi_1/glue/Cu_{99}Bi_1/SiO_2$ sandwich reveal Bi enrichment in the nanocrystalline structure [only the $M\alpha 1$ counts (cts) for Bi were considered].

choose the pure nanocrystalline Cu and the single-crystal (473 K) or liquid (673 and 873 K) Bi as reference states, respectively. As shown in Fig. 3, for temperatures below the grain boundary wetting temperature of Bi, we find negative or vanishing enthalpies of mixing for $\lesssim 2400$ substitutional atoms. For higher grain boundary concentrations, positive values (0.24 ± 0.005 eV/atom; Fig. 3) are detected. Using Ag instead of Bi impurities leads to a qualitatively similar behavior, using single-crystalline Ag as reference state at 673 K; only the number of sites with negative or vanishing heats of mixing is strongly enhanced, thus reflecting a higher solubility of Ag in Cu. Beyond the grain boundary wetting temperature, the heat of mixing of Bi in Cu always remains positive and reaches 0.52 ± 0.005 eV/atom for high enough concentrations (Fig. 3). Within this context it seems necessary, however, to emphasize, that for any of the concentrations or types of grain boundary dopant the enthalpies of mixing remain strictly positive, if a single-crystal Cu reference state is chosen instead of the nanocrystal. This indicates that the presence of grain boundaries is always enthalpically unfavorable—independent of the type of doping.

Assuming that diffusion of Bi impurities within Cu grain boundaries and exchange with the open surface proceed fast enough to ensure thermodynamic equilibrium, we first treat Bi as substituents in a rigid Cu grain boundary matrix. When a grand canonical ensemble is employed for an individual

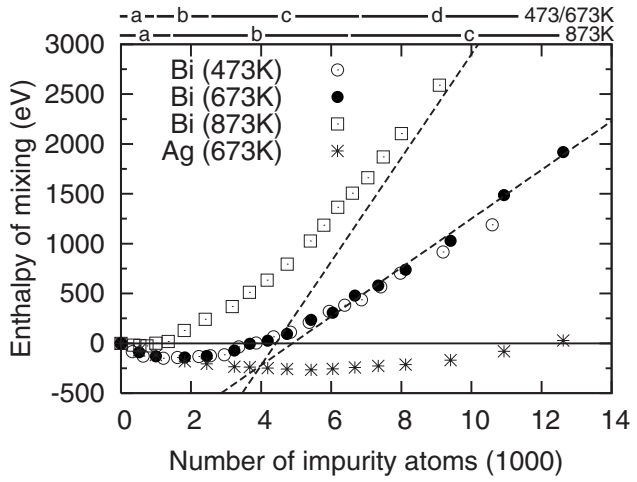

FIG. 3. Enthalpies of mixing for Bi and Ag substitutional impurities, obtained by successively doping the lowest enthalpy substitutional sites within Cu grain boundaries—as a function of temperature. Note the negative heats of mixing at low impurity concentrations, and linear increase at higher concentrations. The total number of grain boundary atoms was determined to be 98 634 atoms. The bars on the very top of the picture indicate the classification of Bi grain boundary substitutional sites by their enthalpies of mixing. All quantities were evaluated after annealing pure Cu cells for 1 ns, followed by additional 20 ps after doping.

grain boundary substitutional site, $\Delta g_i = g_i - \mu$, viz., the difference of the Gibbs free energy of an impurity i, g_i, and the chemical potential μ are the decisive quantities for determining equilibrium concentration.[48] Since the works of Gibbs[49] and (in a more modern formalism) Cahn,[3] it has been known that the chemical potential of a flat surface or interface equals that of the corresponding bulk solid. That is, Δg_i is well approximated by $\Delta h_{mix,i}$, assuming negligible vibrational entropy contributions during mixing. In our simulations performed to obtain $\Delta h_{mix,i}$ (Fig. 3), low-energy positions for substituents were found to appear approximately as pairs of sites, which are located next to each other on different sides of the grain boundary. However, simultaneous occupation of both sites proved to be energetically highly unfavorable. This can be rationalized by the fact that $\Delta h_{mix,i}$ primarily originates from the volume mismatch of Bi in Cu, and consequently can be reduced in portions of the grain boundary with positive volume excess, while it is increased in regions with negative volume excess, e.g., in the presence of another Bi atom. Cast in an equation, this yields for the probability p_i of a single occupied pair of substitutional sites

$$p_i = (1 + 0.5e^{\Delta h_{mix,i}/k_B T})^{-1}. \quad (2)$$

In the following we aim to investigate the growth behavior of Cu nanograins both with and without the presence of Bi or Ag grain boundary dopants directly in MD simulations. To prove the feasibility of these studies within the time scales accessible in MD, we first monitor the temporal evolution of the grain microstructure with an initial diameter of 6 mn in pure Cu (Fig. 4). Clearly significant coarsening occurs already within the first 6 ns at 673 K. This is corroborated by the detailed evaluation of the temporal evolution of the number of grain boundary atoms, N, at three representative temperatures in Fig. 5. We subsequently investigate the impact of dopants on the course of grain growth at 1 ns by substituting Cu with Bi dopants according to the equilibrium distribution of Eq. (2). The latter is realized based on locally resolved enthapies of mixing (Fig. 3); the corresponding Bi concentrations are included in Fig. 5. As shown in Fig. 5, grain growth dramatically slows down for all temperatures investigated upon addition of Bi, viz., the nanograins become stabilized. However, even much lower concentrations of Bi grain boundary dopants than in equilibrium are already suf-

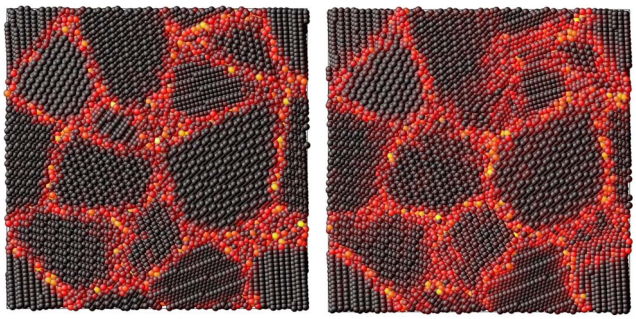

FIG. 4. (Color online) Cross-sectional snapshots through a three-dimensional nanocrystalline Cu simulation cell, using atomistic von Mises shear-strain-invariant color encoding (Ref. 47): Clearly grain boundary migration occurs during annealing at 673 K for 6 ns [(a) 0 ns and (b) 6 ns].

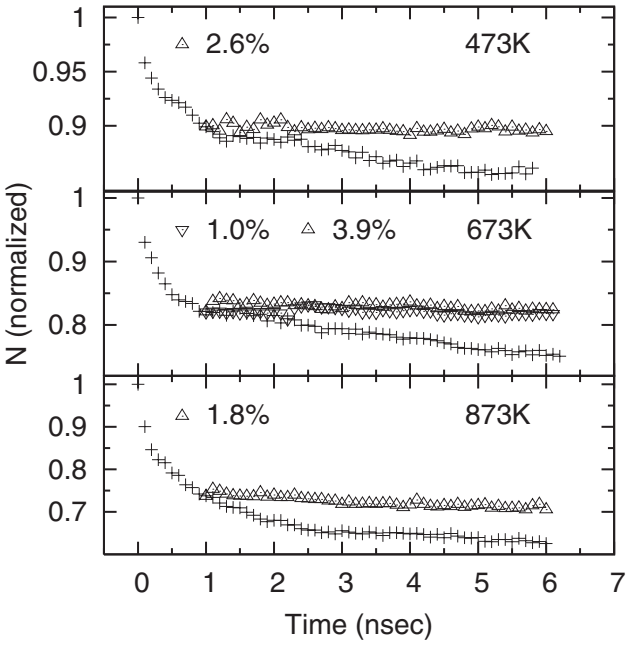

FIG. 5. Modification of Cu grain growth behavior, as represented by the normalized number of grain boundary atoms, N (+ symbols) upon addition of equilibrium (△) grain boundary concentration of Bi as a function of simulation time. For one run at 673 K (▽ symbols) an out-of-equilibrium distribution of Bi was realized, with only type a sites (Fig. 3) being occupied. Grain growth dramatically decelerates in all cases.

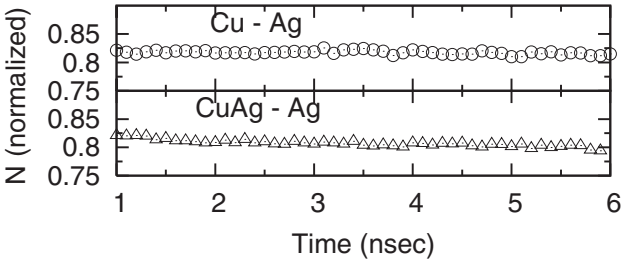

FIG. 6. Deceleration of grain growth at 673 K in the presence of Ag impurities—in similarity to Fig. 5. (○) Equilibrium concentration of Ag impurities (11%) was added only to grain boundaries while the grains themselves remained undoped; (△) equilibrium of Ag impurities was established in grain boundaries (11%) and within the grains (7%), based on the regular solution model.

ficient to greatly inhibit grain growth, if sufficiently low-enthalpy substitutional sites are occupied: As an example, Fig. 5 includes a data set at 673 K with only the type *a* substitutional sites being occupied by Bi. These findings emphasize the key role of low-enthalpy substitutional sites in stabilization of nanograins.

When compared with Cu-Bi, the Cu-Ag system is generally characterized by higher miscibilities and lower enthalpies of mixing, which could be expected to interfere less with grain growth—either by reducing thermodynamical stabilization of grain boundaries or by entailing faster kinetics. However, on the time scales of MD, Ag grain boundary dopants in nanocrystalline Cu inhibit grain coarsening as well (Fig. 6), no matter whether thermal equilibrium is established only in the grain boundaries, or also within the grains. In fact, this finding is not too surprising, after all, in view of the similarities of the enthalpy curves for Bi and Ag substitutes (Fig. 3), which emerges as a key quantity within the present investigation.

By substituting grain boundary atoms randomly [i.e., not following the thermodynamic distribution of Eq. (2)] at 473, 673, and 873 K, respectively, *out-of-equilibrium* Bi or Ag grain boundary concentrations are obtained. Experimentally similar conditions can be envisioned during far-from-equilibrium processing, such as vapor *co*deposition of Cu and Bi or Ag at low substrate temperatures (Fig. 1), rapid quenching, ion bombardment, or ball milling. As the results for 473 K prove to be qualitatively comparable to those at 673 K, we restrict ourselves to 673 and 873 K in the following. Figure 7 shows the response of the microstructure at 673 and 873 K in the absence of open surfaces. For grain boundary concentrations of 25% Bi, grain growth ceases while the number of Bi neighbors of Bi slightly increases (Table I). The latter can be interpreted in terms of Bi precipitation tendencies, which only partially prevail due to the limited time scales of MD. However, at concentrations as high as 50%, our data evaluation indicates an *increase* in grain boundary atoms or a grain shrinkage, which is particularly pronounced at 873 K. At first sight it might be tempting to interpret this behavior in terms of an increase of grain boundary area, viz., a decomposition of grains into smaller subgrains, as predicted thermodynamically for idealized supersaturated systems with large positive heats of mixing in the absence of

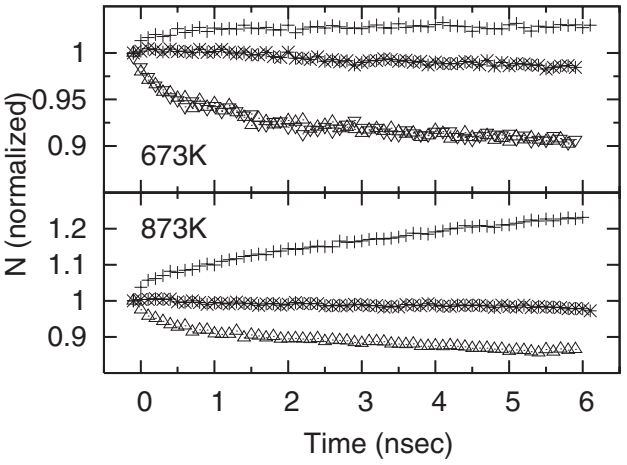

FIG. 7. Grain growth behavior in the presence of supersaturated, randomly doped grain boundaries of pure Cu grains with 25% Bi (∗), 50% Bi (+), and 25% Ag (△) grain boundary dopants. Doping was performed at randomly selected grain boundary sites directly after cell relaxation [not following the thermodynamic distribution of Eq. (2)], resulting in out-of-equilibrium grain boundary doping. Additional presence of an equibrium concentration of Ag substituents (≈7% at 673 K) within the Cu grains for samples with 25% Ag grain boundary dopants (▽) did not significantly influence grain growth behavior, when compared with undopeded grains, as indicated by overlapping △ and ▽ symbols in the top part of the figure.

precipitation and surface segregation.[5] However, a concurrent decrease of Bi in the neighboring shell of Bi atoms clearly suggests the presence of mixing (viz., alloying) effects in the grain boundary region. In fact, this simulational observation is consistent with experiments, which report grain boundary alloying effects in the grain boundary wetting regime at temperatures as high as 873 K.[22,23] Visual inspection additionally corroborates that grain shrinkage at 873 K occurs only due to an increase of grain boundary width during formation of a grain boundary alloy phase, while formation of additional grain boundary area is not observed. In fact, even when creation of additional grain boundaries should become thermodynamically favorable, e.g., in the presence of a negative grain boundary free energy (see Sec. V), we speculate about additional stress-related enthalpy contributions, which constitute high-enthalpy barriers for activation.[50]

Surprisingly, sufficiently high increases of Ag grain boundary concentrations at randomly selected grain bound-

TABLE I. Compositional changes within the neighboring shell of Bi, as expressed in number of Bi neighbors. Increases and decreases are indications of precipitation and mixing tendencies, respectively.

T (K)	673		873	
Bi content (%)	25	50	25	50
No. of Bi neighbors of Bi at 0 ns	2.26	3.51	2.23	3.41
No. of Bi neighbors of Bi at 6 ns	2.41	3.60	2.40	3.08

ary sites beyond thermal equilibrium turn out to be incapable of stabilizing Cu nanograins, as is visible by comparing Fig. 5 with Fig. 7. In fact, visual inspections of cross sections of simulation cells at temperatures as low as 473 K indicate that Ag, like Cu, atoms are equally involved in the transport processes that lead to grain coarsening. Hereby, the grain boundary segregation layer either spreads by successively incorporating Ag into surrounding crystallites, or shows precipitation tendencies, which even seem to be enhanced over the effects of Bi—presumably due to the enhanced mobility of Ag.

V. DISCUSSION

In the following section we aim to discuss the physics of grain boundary stabilization in detail by employing thermodynamic and kinetic concepts. Here we particularly focus on Bi and extend our considerations to Ag where appropriate. To estimate the Gibbs free energy change ΔG_{mix} due to the presence of Bi dopants within Cu grain boundaries, we group all possible substitutional sites into i subsets of N_i^0 pairs of sites with equivalent enthalpies of mixing $\Delta h_{mix,i}$. Noting that G is an extensive quantity and assuming that each pair can maximally be occupied by one dopant results in

$$\Delta G_{mix} = \sum_i \left\{ N_i \Delta h_{mix,i} - k_B T \ln \left[2^{N_i} \binom{N_i^0}{N_i} \right] \right\} \tag{3}$$

where N_i denotes the number of dopants in subset i. Application of the Stirling approximation (e.g., Ref. 51) yields

$$\Delta G_{mix} = \sum_i \left[N_i \Delta h_{mix,i} - k_B T N_i \ln 2 - k_B T N_i \ln \left(\frac{N_i}{N_i^0} \right) - k_B T (N_i^0 - N_i) \ln \left(\frac{N_i^0 - N_i}{N_i^0} \right) \right]. \tag{4}$$

Minimizing ΔG_{mix} with respect to N_i leads to a distribution of impurity atoms in accordance with Eq. (2) with $p_i = N_i / N_i^0$, as expected. We proceed in estimating ΔG_{mix} by noting that grain boundary substitutional sites (Bi for Cu) can roughly be classified into distinct categories ($i = a, b, \ldots$ in Fig. 3), according to their enthalpies of mixing (e.g., $\Delta h_{mix,a} \approx -0.16$ eV, $\Delta h_{mix,b} \approx 0$ eV, $\Delta h_{mix,c} \approx 0.12$ eV, and $\Delta h_{mix,d} \approx 0.24$ eV for 473 and 673 K). When these results are inserted in a combination of Eqs. (2) and (4), the Gibbs free energies of grain boundary mixing are readily calculated (Table II).

Gibbs free energy changes associated with alloying Bi solutes into Cu grain boundaries are manifested in modifications of the average grain boundary free energy $\langle \sigma \rangle$. Within this context, it is necessary to issue a major caveat on the appropriate choice of a reference system for calculation of $\langle \Delta \sigma \rangle$ upon alloying, where boundary conditions play a crucial role: In previous investigations[5,6,10] on idealized single-phase closed systems, $\langle \Delta \sigma \rangle$ was shown to be governed by the differences of the Gibbs free energies of mixing in the grain boundary and matrix, respectively, viz., the segregation Gibbs free energy. This is primarily based on the fact that grain boundary segregation and grain growth occur at the expense of the solute concentration in the matrix, and vice versa. Presently, however, we deal with an *open* system, where thermodynamic equilibrium and particle exchange of solutes in grain boundaries and the surface play crucial roles. In fact, solution in the matrix remains enthalpically highly unfavorable, and consequently can be considered negligible for CuBi. Assuming free exchange of dopants with the surface, the modification of grain boundary free energy becomes $\langle \Delta \sigma \rangle = \Delta G_{mix} / A$, where A denotes the grain boundary area. From the results shown in Table II, it becomes clear that an overall thermodynamic stabilization of Cu grain boundaries cannot occur under these conditions; in fact, there remains an overall driving force for grain growth even in the presence of Bi, as indicated by $\langle \sigma_0 \rangle + \langle \Delta \sigma \rangle > 0$.

However, Bi dopants are able to locally reduce grain boundary free energies within subset a of substitutional sites, $\sigma_{0,a} + \Delta \sigma_a$, until below zero for all temperatures investigated. Competition between locally negative and positive grain boundary free energies thus leads to counteracting driving forces for grain shrinkage and growth, respectively, and thus frustration of grain growth in the sense of a metastable equilibrium. Surely, strongly restricted kinetics plays a key role in preserving metastability. That is, high activation barriers have to be overcome to move and eliminate grain boundaries, as type a substitutional sites generally cannot be expected to be preserved during grain boundary migration or elimination. Thus, the requirement of thermal activation for

TABLE II. (i) Average Cu grain boundary free energy before doping $\langle \sigma_0 \rangle$, (ii) reduction of Gibbs free energy upon addition of the equilibrium concentration of Bi grain boundary dopants [following Eq. (2)], ΔG_{mix}, (iii) the corresponding average change of grain boundary free energy $\langle \Delta \sigma \rangle$, (iv) average grain boundary free energy for type a sites before doping, $\sigma_{0,a}$, and (v) the change of grain boundary free energy in type a sites upon equilibrium doping, $\Delta \sigma_a$. All quantities were evaluated after annealing the pure Cu cells for 1 ns, followed by an additional 20 ps after grain boundary doping. While calculation of $\langle \sigma_0 \rangle$ was based on a comparison of the total enthalpies of single and polycrystalline cells, $\sigma_{0,a}$ was determined from the elevated binding enthalpies of individual grain boundary atoms within subset a. In all cases, the grain boundary entropies were estimated from the universal equation of state (Ref. 52), using the materials parameters of Cu (Ref. 53) and a grain boundary free volume as extracted directly from MD. Due to a communal entropy contribution to the liquid Bi reference state at 673 K, slightly increased values for $\langle \Delta \sigma \rangle$ and $\Delta \sigma_a$ have to be expected by some tens of meV/atom (based on the typical entropies of fusion). Vice versa, a slight decrease at 873 K seems plausible due to communal entropy contributions during grain boundary wetting.

	T (K)		
	473	673	873
$\langle \sigma_0 \rangle$ (meV/atom)	157	145	135
ΔG_{mix} (eV)	−238.4	−378.3	−194.7
$\langle \Delta \sigma \rangle$ (meV/atom)	−2.4	−3.8	−2.0
$\sigma_{0,a}$ (meV/atom)	108	63	55
$\Delta \sigma_a$ (meV/atom)	−189	−202	−97

grain boundary migration can clearly be interpreted in terms of a drag force on the grain boundaries, i.e., our general thermodynamic treatment is capable of naturally incorporating the old notion of solute drag.[4]

In adition to these thermodynamic considerations, two additional simulation results shown in Sec. IV can strongly corroborate the key role of low-enthalpy substitutional sites for nanograin stabilization. (i) As shown in Fig. 5 a very low density of Bi substituents in Cu grain boundaries (only 1% of the grain boundary atoms, or 0.2% total) is already sufficient to inhibit grain growth, if the Bi substitutes are only placed on type *a* substitutional sites. (ii) In our simulations of Ag dopants in Cu or CuAg nanocrystallites, grain growth is decelerated only in the case of an equilibrium distribution of Ag grain boundary dopants (filling primarily type *a* sites; Fig. 6), while much higher random occupation densities of grain boundary sites (Fig. 7) cannot decelerate grain growth, when compared with pure Cu in the absence of dopants (Fig. 5). This again emphasizes the role of low-enthalpy grain boundary substitutional sites in nanostructure stabilization. In contrast, in the presence of random Bi grain boundary dopants, the latter effect is not observed, presumably due to the much higher enthalpy of mixing of the bulk phases. In addition, finding (ii) is instructive also from a simulation point of view, as it generally proves the feasibility of dopant transport in Cu on the time scale of MD.

VI. CONCLUSION

We have investigated the physical mechanisms responsible for grain boundary stabilization by dopants in the presence of open surfaces, using the model system CuBi in a combined experimental-simulational study. During annealing of a $Cu_{99}Bi_1$ thin film at 473 K, we find experimentally the stabilization of Cu nanograins within Bi-rich nanocrystalline layers at the surface and $SiO_2/Cu_{99}Bi_1$ interface. From MD simulations we extract the grain boundary enthalpies of mixing, and monitor the evolution of grain size in the absence and presence of various concentrations of Bi during annealing—in comparison with Ag. At equilibrium Bi concentrations—and even below—we find that grain growth ceases for temperatures up to 873 K, while higher out-of-equilibrium concentrations can result in the formation of precipitates and a grain boundary phase. Within the picture of grain boundary free energy, grain stabilization can be interpreted as the occurrence of locally negative grain boundary free energy, which leads to frustration of grain growth, while the average overall grain boundary free energy always remains positive. Our full thermodynamic treatment naturally incorporates the traditional notion of solute drag, and should be applicable to any nanosystem with sufficiently large segregation of the dopants.

ACKNOWLEDGMENTS

We are indebted to M. Seibt and co-workers, Universität Göttingen, Germany, for support with TEM characterization. Financial support by the German DFG, SFB 602, TP B3, as well as a grant of computing time by the Gesellschaft für wissenschaftliche Datenverarbeitung Göttingen (GWDG), Germany, are gratefully acknowledged.

*Author to whom correspondence should be addressed. smayr@uni-goettingen.de

[1] R. Waser, *Nanoelectronics and Information Technology* (Wiley-VCH, Weinheim, 2005).
[2] H. Gleiter, Acta Mater. **48**, 1 (2000).
[3] J. W. Cahn, in *Interfacial Segregation*, edited by W. C. Johnson and J. M. Blakeley (American Society for Metals, Metals Park, OH, 1979), p. 3.
[4] K. Lücke and K. Detert, Acta Metall. **5**, 628 (1957).
[5] J. Weissmuller, Nanostruct. Mater. **3**, 261 (1993).
[6] J. Weissmuller, J. Mater. Res. **9**, 4 (1994).
[7] Z. Q. Gao and B. Fultz, Nanostruct. Mater. **4**, 939 (1994).
[8] J. Weissmüller, J. Löffler, and M. Kleber, Nanostruct. Mater. **6**, 105 (1995).
[9] K. W. Liu and M. Mücklich, Acta Mater. **49**, 395 (2001).
[10] R. Kirchheim, Acta Mater. **50**, 413 (2001).
[11] W. Hampe, Z. Berg-, Hütten- und Salinewesen **23**, 93 (1874).
[12] T. B. Massalski, *Binary Alloy Phase Diagrams* (American Society for Metals, Metals Park, OH, 1986).
[13] L. S. Chang, B. B. Straumal, E. Rabkin, W. Gust, and F. Sommer, J. Phase Equilib. **18**, 128 (1997).
[14] U. Alber, H. Müllejans, and M. Rühle, Acta Mater. **47**, 4047 (1999).
[15] G. A. Lopez, W. W. Gust, and E. J. Mittemeijer, Scr. Mater. **49**, 747 (2003).
[16] B. Blum, M. Menyhard, D. E. Luzzi, and C. J. McMahon, Scr. Metall. Mater. **24**, 2169 (1990).
[17] T. Muschnik, W. Laub, U. Wolf, M. W. Finnis, and W. Gust, Acta Metall. Mater. **41**, 2163 (1993).
[18] B. B. Straumal, S. A. Polyakov, E. Bischoff, W. Gust, and B. Baretzky, Acta Mater. **53**, 247 (2005).
[19] W. Sigle, L. S. Chang, and W. Gust, Philos. Mag. A **82**, 1595 (2002).
[20] G. Duscher, M. F. Chrisholm, U. Alber, and M. Rühle, Nat. Mater. **3**, 621 (2004).
[21] R. Schwinfest, A. T. Paxton, and M. W. Finnis, Nature (London) **432**, 1008 (2004).
[22] L. S. Chang, E. Rabkin, B. B. Straumal, B. Baretzky, and W. Gust, Acta Mater. **47**, 4041 (1999).
[23] S. Divinski, M. Lohmann, C. Herzig, B. Straumal, B. Baretzky, and W. Gust, Phys. Rev. B **71**, 104104 (2005).
[24] M. W. Finnis and J. E. Sinclair, Philos. Mag. A **50**, 45 (1984).
[25] V. Vitek, G. J. Ackland, M. Menyhard, and M. Yan, in *Interfaces: Structure and Properties*, edited by S. Ranganathan, C. S. Pande, B. B. Rath, and D. A. Smith (Trans Tech Publications, New Delhi, 1993), p. 3.
[26] M. Yan, M. Sob, D. E. Luzzi, V. Vitek, G. J. Ackland, M. Methfessel, and C. O. Rodriguez, Phys. Rev. B **47**, 5571 (1993).
[27] R. Siegl, M. Yan, and V. Vitek, Modell. Simul. Mater. Sci. Eng. **5**, 105 (1997).

[28] P. C. Millett, R. P. Selvam, S. Bansal, and A. Saxena, Acta Mater. **53**, 3671 (2005).
[29] S. G. Mayr, M. Moske, and K. Samwer, Phys. Rev. B **60**, 16950 (1999).
[30] H. Höfler, R. S. Averback, and H. Hahn, J. Appl. Phys. **74**, 3832 (1993).
[31] C. Streng, K. Samwer, and S. G. Mayr, Appl. Phys. Lett. **81**, 5135 (2002).
[32] D. Bedorf and S. G. Mayr (unpublished); D. Bedorf, Diploma Thesis, University of Göttingen, 2006.
[33] M. S. Daw and M. I. Baskes, Phys. Rev. Lett. **50**, 1285 (1983).
[34] S. M. Foiles, M. I. Baskes, and M. S. Daw, Phys. Rev. B **33**, 7983 (1986).
[35] J. P. Rogers, P. Wynblatt, S. M. Foiles, and M. I. Baskes, Acta Metall. Mater. **38**, 177 (1990).
[36] D. Udler and D. N. Seidman, Phys. Rev. B **54**, R11133 (1996).
[37] H. J. C. Berendsen, J. P. M. Postma, W. F. van Gunsteren, A. DiNola, and J. R. Haak, J. Chem. Phys. **81**, 3684 (1984).
[38] Employing a Nosé-Hoover thermostat (Refs. 39 and 40) instead did not lead to significantly different results in test runs.
[39] S. Nosé, Mol. Phys. **52**, 255 (1984).
[40] W. G. Hoover, Phys. Rev. A **31**, 1695 (1985).
[41] G. F. Voronoi, J. Reine Angew. Math. **135**, 67 (1909).
[42] In the present potentials the size mismatch is the key origin of the heat of mixing, as, e.g., derived in a semiempirical way by Miedema and co-workers (Ref. 43).
[43] A. R. Miedema, Philips Tech. Rev. **36**, 217 (1976).
[44] H. Zhu, R. S. Averback, and M. Nastasi, Philos. Mag. A **71**, 735 (1995).
[45] Polycrystals generated by Voronoi constructions are initially composed of grains with highly unrelaxed but uncurved grain boundaries. With the driving force for grain growth thus being greatly absent, grain boundary relaxation or densification is the predominant mechanism. In the course of relaxation also a grain boundary curvature develops, presumably initiated from the triple points.
[46] For example, R. T. De Hoff and F. N. Rhines, *Quantitative Microscopy* (McGraw-Hill, New York, 1968).
[47] J. Li, Modell. Simul. Mater. Sci. Eng. **11**, 173 (2003).
[48] The index i refers to a classification of all pairs of substitutional sites according to their enthalpy of mixing $\Delta h_{mix,i}$.
[49] J. W. Gibbs, *The Collected Works* (Yale University Press, New Haven, CT, 1957), Vol. 1, p. 320.
[50] However, external forcing, such as ball milling or ion irradiation, might help to overcome these barriers.
[51] I. Prigogine and R. Defay, *Chemische Thermodynamik* (VEB Deutscher Verlag für Grundstoffindustrie, Leipzig, 1962).
[52] H. J. Fecht, Phys. Rev. Lett. **65**, 610 (1990).
[53] J. H. Rose, J. R. Smith, F. Guinea, and J. Ferrante, Phys. Rev. B **29**, 2963 (1984).